Identification of an autophagy-related prognostic signature in head neck squamous cell carcinoma

Yue Jiang
Nanjing Medical University
Yuanyuan Li
Nanjing Medical University
Han Ge
Nanjing Medical University
Yaping Wu
Nanjing Medical University
Yuchao Zhang
Nanjing Medical University
Songsong Guo
Nanjing Medical University
Ping Zhang
Nanjing Medical University
Jie Cheng
Nanjing Medical University
Yanling Wang (wangyanling@njmu.edu.cn)
Nanjing Medical University https://orcid.org/0000-0003-1922-6950

Primary research

Keywords: Head neck squamous cell carcinoma, Autophagy-related genes, Prognosis, Signature, TCGA

Posted Date: December 10th, 2020

DOI: https://doi.org/10.21203/rs.3.rs-123004/v1

Abstract

Background

Autophagy-related genes (ARGs) have been significantly implicated in tumorigenesis and served as promising prognostic biomarkers for human cancer. Hence, this study was aimed to develop an ARGs-based prognostic signature for head neck squamous cell carcinoma (HNSCC).

Methods

Prognostic ARG candidates were identified by univariate and multivariate Cox regression analysis in training set (TCGA-HNSC) and incorporated into a 3-ARGs (EGFR, FADD, PARK2) prognostic signature, which further verified in two independent validation cohorts (GSE41613 and GSE42743). Kaplan-Meier plots, Cox regression analyses and receiver operating characteristics curves (ROC) were employed to evaluate the prognostic prediction of 3-ARGs signature. Differential expression of these 3 ARG between cancer and normal counterparts as well as their associations with autophagy markers were assessed using Human Protein Profiles dataset.

Results

Patients with high-risk score had significantly inferior overall survival. Multivariate survival analyses revealed that 3-ARGs signature could be an independent prognostic factor. ROC analyses revealed the high predictive accuracy and sensitivity of 3-ARGs signature. Increased expression of EGFR, FADD, PARK2 were found in HNSCC samples and their expression significantly correlated with levels of ATG5, Beclin1 and LC3.

Conclusions

Our results reveal that 3-ARGs signature is a powerful prognostic biomarker for HNSCC, which could be integrated into current prognostic regime to realize individualized outcome prediction.

Introduction

Head neck squamous cell carcinoma (HNSCC) represents the sixth most common malignancy worldwide with an estimated 600,000 new cases and 350,000 cancer-related deaths worldwide each year.[1] Until now, the well-established etiological risk factors associated with this lethal malignancy include alcohol, smoking and human papillomavirus infection (HPV). Previous intensive efforts were attempted to dissect the genetic, epigenetic and environmental factors that initiated HNSCC tumorigenesis.[2] Considerable advances in multidisciplinary treatment regimen for HNSCC including surgery, chemotherapy, radiotherapy and immunotherapy has remarkably improved life expectancy and quality of life among

patients diagnosed at early stage.[3, 4] However, the mortality rates of HNSCC are still high and the 5-year survival ratios remain approximately 60 percent and even worse in those with advanced diseases.[1, 5] Multiple clinicopathological parameters such as depth of invasion, clinical stage, locoregional relapse and cervical lymph node metastasis have been recognized as the well-established factors dictating patient prognosis. Nevertheless, these abovementioned prognostic predictors as well as routinely used TNM staging system are not reliable and optimal for patient stratification and prognostic prediction is owing to the fact that patients within the same categories substantially varied in survival.[6] Therefore, novel biomarkers with adequate performance and clinical convenience are urgent to be identified, which are fundamental for improving treatment outcomes.

Autophagy is a fundamental process to maintain intracellular homeostasis by which cells target intracellular components for degradation in the lysosome under conditions of hypoxia, oxidative stress or nutrient deprivation.[7, 8] Although it is originally regarded as a “bulk degradation” process, accumulating evidence has demonstrated that autophagy is a highly selective quality-control mechanism that modulates the abundance of specific organelles and proteins. Moreover, when it goes awry, it has contributed to numerous pathological processes including cardiomyopathy, neurodegenerative diseases and cancer.[9, 10] In various cancers, the roles of autophagy substantially vary and might be stage or context-specific. [11] In the early stage of cancer, autophagy promotes degradation of damaged organelles or proteins with assistance to relieve cellular damage and chromosome instability, which suppress cancer progression. On the contrary, when cancer has formed, cancer cells strive to survive and progress in the harsh environment under the autophagy assistance.[12, 13] Several studies have reported that autophagy plays an indispensable role underlying cancer recurrence, metastasis and therapeutic resistance.[14, 15] In HNSCC samples, expression levels of several components of autophagy and its regulators like p62 and LC3-II have been found to be significantly associated with patient survival.[16, 17] Noticeably, integrating multiple autophagy genes into a single prognostic signature have shown robust prognostic significance in several human cancer as compared to biomarkers based on individual gene. Novel prognostic signatures by integrating 5 or 9 autophagy-related genes (ARGs) have been developed and validated in lung cancer and breast cancer.[18, 19] These signatures robustly estimated patients’ survival and improved the individualized outcome prediction, thus suggesting translational potentials. Hence, to reveal the roles of ARGs and their prognostic values in HNSCC is of great interests and clinical benefits.

In the present study, we aimed to develop a novel ARGs-based prognostic signature for HNSCC via an integrative bioinformatics approach using gene profiling data and clinicopathological information from publicly available datasets. A 3-ARGs prognostic signature accurately predicting patient survival was developed and further validated in two other independent patient cohorts.

Materials And Methods

Dataset screening and data processing

The 232 autophagy-related genes (ARGs) were extracted from Human Autophagy Database (HADb, http://www.autophagy.lu/index.html) which is an autophagy-dedicated database applied to reserve human genes associated with autophagy. The FPKM RNA-sequencing data and clinical characteristics of HNSCC samples (training cohort) were downloaded from TCGA data portal (https://cancergenome.nih.gov). Two independent HNSCC datasets GSE41613 and GSE42743 were obtained from Gene Expression Omnibus (GEO, https://www.ncbi.nlm.nih.gov/gds/) and selected as validation cohorts. The Robust Multiarray Average method was used to normalize these raw datasets. When more than one probe matched the same gene ID, the probe with the largest expression value was used. Limma package in R statistical software was applied to estimate differentially expressed ARGs between HNSCC and non-tumor samples. Genes exhibiting at least 2-fold changes and *P* value less than 0.05 were selected as differentially expressed ARGs.

Functional enrichment analysis of differentially expressed ARGs

Functional enrichment analyses including Gene ontology (GO) and Kyoto Encyclopedia of Genes and Genomes (KEGG) analyses were performed to characterize major biological attributes those differentially expressed ARGs. The Database for Annotation, Visualization, and Integrated Discovery (DAVID, https://david.ncifcrf.gov/) was applied to identify enriched GO and KEGG themes. To provide high-dimensional information, the GOplot package of R was utilized to visualize these enrichment terms.

Identification of prognostic ARGs

These selected ARGs with significant differential expression between HNSCC and non-tumor samples were analyzed in the univariate Cox regression analysis based on computing environment R with Survival package. After survival analysis, differentially expressed ARGs with *P* value less than 0.05 were identified as prognostic candidates. Moreover, to improve the feasibility and reliability of prognostic prediction of these ARGs, significantly survival-related autophagy genes were selected and further subjected to a multivariate Cox regression analysis to rule out those genes which were unable to serve as independent indicators in prognosis monitoring.

Construction and validation of ARG-based prognostic models

A risk score formula was established through calculating individual prognostic ARGs and weighting their estimated regression coefficients in the multivariable Cox regression analysis using the training dataset. Based on this formula, risk score for each patient in the training set was estimated. A receiver operating characteristic (ROC) curve was plotted using R with survival ROC package. The optimal cut-off point for the risk score was identified with maximal sensitivity and specificity of the ROC curve. Kaplan-Meier analyses and Log-rank test were used to compare the survival differences between patients in the low and high risk subgroups stratified according to the pre-set optimal cut-off point. Subsequently, further validation of this prognostic signature was conducted by fitting in two independent validation datasets.

Statistical analysis

Human Protein Profiles (https://www.proteinatlas.org) was used to obtain IHC images and differential expression of ARGs between normal and tumor tissue. Univariate and multivariate prognostic analyses were performed by Cox proportional hazards regression model. HRs with 95% confidence intervals (CIs) were calculated as estimates of the correlations. ROC curves were plotted to define sensitivity and specificity of risk score by calculating the area under the curves (AUC). Rates of survival were calculated by the Kaplan-Meier method and compared to Log-rank test based on ROC-derived optimal cutoff point. Relationship analysis was evaluated by Pearson's test as suggested. *P* values less than 0.05 were considered statistically significant. Statistical analyses were performed using IBM SPSS 22.0 software (SPSS Inc, Chicago, IL), GraphPad Prism 7 (GraphPad Software, La Jolla, CA) and R 3.6.1.

Results

Identification and Functional annotation of differentially expressed ARGs in HNSCC

All clinicopathological and RNA-seq data in a total of 502 HNSCC and 44 non-tumor samples were retrieved from TCGA portal. The expression of all ARGs in these samples were calculated and compared. Then, 28 up-regulated and 10 down-regulated ARGs (P <0.05, fold change >2.0) were identified in tumor samples compared to non-tumor counterparts (**Fig.1A, B**). In detail, the expression patterns of these 38 differentially expressed ARGs were visualized in box plots (**Fig.1C**).

To gain insights into the biological functions of these differentially expressed ARGs in HNSCC, we performed gene annotation analysis using DAVID platform. As expected, our results indicated that these genes were significantly enriched in functional categories involved in regulation of apoptotic signaling and autophagy (**Fig.2**). Moreover, as displayed in **Fig.3**, KEGG pathway enrichment analysis revealed that these genes were significantly associated with apoptosis, EGFR tyrosine kinase inhibitor/Platinum resistance, HPV infection, and ErbB signaling pathway, et al. These results suggest that these ARGs might contribute to HNSCC tumorigenesis through various biological pathways and processes, and also highlight the incompletely known roles of autophagy in HNSCC initiation and progression.

Identification of prognostic ARG candidates in HNSCC

Among 546 HNSCC samples in TCGA, 499 patients had clinical follow-up information available and then enrolled for prognostic analyses. To explore the potential associations between ARGs and overall survival (OS) in patients with HNSCC, univariate Cox proportional hazards regression analysis was applied to screen the prognosis-related ARGs. Our results revealed that the abundance of 8 differentially expressed ARGs (BAK1, CXCR4, EGFR, NKX2-3, FADD, CDKN2A, CTSL1 and PARK2) were remarkably correlated with overall survival with P values less than 0.05 (**Fig.4**). In order to enhance the robustness, these 8 candidates were further subjected for multivariate Cox regression analyses and subsequently 3 ARGs including EGFR, FADD, PARK2 were consistently identified as independent prognostic factors and further included to develop a prognostic signature (**Fig.5A**).

The 3-ARGs prognostic signature predicts survival of patients with HNSCC

A risk score formula based on the expression level and weighted by coefficient of these three prognostic ARGs was generated as follows: risk score = (0.09646 × expression level of EGFR) + (0.18189 × expression level of FADD) + (0.52452 × expression level of PARK2). Subsequently, ROC analysis was performed to estimate the sensitivity and specificity of this 3-ARGs prognostic signature in survival prediction. The optimal cut-off point was selected as 1.045 which had the maximal sensitivity and specificity (**Fig.5B**). Accordingly, patients in the training cohort (TCGA-HNSCC) were stratified into subgroups with high risk score (n=191) or low risk score (n=308). The Kaplan-Meier analysis revealed that patients with increased scores had markedly inferior survival as compared with those with low scores (*P*< 0.0001, **Fig.6A**). As shown in **Fig.6B-D**, the survival among patients, the distribution of risk score and expression of individual ARGs in HNSCC samples were shown in detail.

Validation of the 3-ARGs prognostic signature for survival prediction

We next validated the predictive value of this 3-ARGs prognostic signature using other two independent HNSCC datasets (GSE41613 and GSE42743). Utilizing the established risk score formula, patients in these two cohorts were classified into high-risk and low-risk subgroups. Consistent with the results from the training cohort, patients with high scores had significantly inferior overall survival compared with those with low scores in the GSE41613 cohort (*P*=0.013, **Fig.7A**) and GSE42743 cohort (*P* =0.034, **Fig.7C**), respectively. Subsequently, ROC curve was plotted to evaluate the prognostic accuracy of this 3-ARGs prognostic signature, presenting AUC values 0.673 and 0.627 in these two datasets, respectively **(Fig.7B, D)**.

Univariate and multivariate prognostic analyses of 3-ARGs signature in HNSCC

As shown in **Table 1**, we employed univariate Cox regression analyses to substantiate the prognostic values of 3-ARGs signature and revealed that 3-ARGs signature risk score was remarkably associated with overall survival of patient in the TCGA cohort (HR, 1.845; 95% CI, 1.410-2.416; *P*<0.001). As anticipated, some well-established prognostic parameters including tumor size, pathological grade and cervical node metastasis were also identified as prognostic predictors. Furthermore, to rule out other confounding factors, we performed multivariate Cox regression analyses and found that this 3-ARGs prognostic signature was identified as an independent prognostic predictor for overall survival in TCGA-HNSCC cohort (HR, 1.735; 95% CI, 1.282-2.348; *P* < 0.001).

Expression of EGFR, FADD and PARK2 in HNSCC and their correlations with autophagy markers

Finally, the expression of three identified ARGs (EGFR, FADD and PARK2) in clinical specimens from Human Protein Profiles (https://www.proteinatlas.org) was retrieved and compared with normal counterparts. Significantly higher expression of these genes in HNSCC tissue was observed (**Fig.8A**). Then, to further understand the associations of three genes and autophagy, we analyzed the correlation between the expression of three candidate genes and three well-established autophagy markers (ATG5, Beclin1 and LC3). Noticeably, significant associations between 3 genes and autophagy markers were identified (**Fig.8B**). In addition, Kaplan-Meier analyses revealed that patients with increased expression of

EGFR and FADD had markedly inferior survival as compared with those with low expression, respectively (*P*= 0.0016 and 0.0043), while PARK2 shown no prognosis significance (*P*=0.28) (**Fig.8C**).

Discussion

HNSCC is a heterogeneous group of carcinomas driven by aberrant alternations of genetic, epigenetic, and environmental factors. Clinical outcomes are substantially varied among patients largely due to tumor heterogeneity.[20] The dismal long-term survival rates and the paucity of powerful prognostic tools for HNSCC highlighted the urgent need to identify novel promising biomarkers with optimal abilities to guide treatment selection and prognostic management. Due to tremendous advancement of high-throughput technologies like genome-wide RNA sequencing, gene profiling coupled with robust statistical algorithms has become an attractive strategy to screen molecular biomarkers for cancer diagnostics and therapeutics.[21–23] Accumulating evidence has revealed that autophagy plays profound roles during diverse stages of tumorigenesis across human cancers including HNSCC.[24] Here, we identified critical ARGs differentially expressed in HNSCC samples and developed a novel ARGs based signature to predict prognosis with adequate performance via an integrative bioinformatics approach.

Several lines of evidence have increasingly indicated that genetic mutations, aberrant expression and regulation of components involved in autophagy have intricately linked to tumor predisposition, initiation and progression. We previously conducted a case-control study to analyze 11 tagging single nucleotide polymorphisms of three core autophagosome formation genes (ATG5, ATG12 and ATG16L1) in 576 HNSCC cases and 1552 healthy controls and found that ATG12 eQTL SNP rs26537 contributed to ATG expression and associated with increased risk of HNSCC in Chinese population.[25] Several components of autophagy such as p62 and LC3-II have been identified to be significantly upregulated in HNSCC and associated with patient survival.[16, 17] Moreover, aberrations in pathways linked to autophagy have been unveiled to fuel HNSCC initiation and progression. For example, PI3K/AKT/mTOR pathway acts a survival mechanism for HNSCC in part by modulating autophagy. Therapeutic targeting this pathway has undergone preclinical evaluation and shown promising results.[26] Here, we comprehensively exploited the high-throughput RNA-seq data from TCGA-HNSCC database and identified critical ARGs with prognostic significance involved in HNSCC. Functional annotations of these ARGs revealed their enrichment in apoptosis regulation, autophagy and ERBB2 signaling pathway, thus supporting their roles responsible for HSNCC development. Indeed, ERBB2 signaling have been linked to autophagy during tumorigenesis.[27] Together, our results support that dysregulated expression of autophagy contributes to HNSCC development, although its roles were highly complex than originally expected. Further in-depth exploration of autophagy underlying HNSCC tumorigenesis is warranted.

Accumulating evidence has shown that several individual ARGs and gene signatures integrating multiple ARGs have prognostic values in multiple cancers. ARGs-based prognostic signatures have been constructed in breast, colorectal, lung cancer and glioblastoma which display robustness and superior performance in prognostic prediction. [22, 28, 29] Here we constructed and validated a 3-ARGs based prognostic signature for HNSCC which was able to stratify patients into subgroups with favorable or

inferior survival. Notably, constitutive components of these signatures remarkably varied and rarely overlapped. We reasoned that this was in line with previous notions that the components of autophagy hijacked by cancer for its progression were quite complex and their roles were highly context-dependent. [30]

In our study, we identified three autophagy-related genes (EGFR, FADD and PARK2) which were associated with HNSCC survival. In particular, EGFR, one of three ARG members in our signature, has been demonstrated to be intricately involved in autophagy in human cancer including HNSCC, which largely depends on its subcellular location and kinase activity. [31] Moreover, targeting EGFR-mediated autophagy has become an attractive strategy for cancer therapeutics. [32] Consistent with previous findings that higher EGFR expression associated with tumor malignant features and patient survival, our data reinforce the idea that activated EGFR signaling represents one of the key molecular features of HNSCC and critically involved in its development at least in part by modulating autophagy. [33] Regarding the gene FADD, previous studies have suggested that overexpressed FADD is associated with regional and distant metastasis in HNSCC.[34] Moreover, recent studies demonstrated that FADD amplification and high expression of FADD were closely relevant with inferior overall survival in HNSCC, especially when both events occur together.[35, 36] PARK2 ectopic expression has been reported as a tumor suppressor gene which mitigates proliferation of tumor cells in various malignancies including colorectal cancer, glioma and non-small-cell lung cancer.[37–39] Here, in order to validate the expression of three identified novel genes (EGFR, FADD and PARK2), we used the Human Protein Atlas and validated the expression difference of the proteins encoded by three identified novel genes between normal and HNSCC tissues. What's more, three candidate genes were identified significant association with acknowledged autophagy key genes. However, much work is still needed to pinpoint the accurate functions of EGFR, FADD and PARK2 in autophagy at diverse stages of HNSCC.

Tremendous progress in high-throughput profiling techniques enables us to capture the whole picture of expression of genes in a genome-wide scale and generate prognostic signatures by integrating multiple genes in human cancer. We and other previously developed several types of prognostic signatures were based on mRNA, miRNA, lncRNA and alternative splicing for HNSCC. [21, 40, 41] Consistent with previous findings, our 3-ARGs signature robustly stratified patients into subgroups with favorable or inferior survival and served as a novel independent prognostic factor affecting patient survival. [22, 29] This 3-ARGs prognostic signature might facilitate patient counseling, decision-making regarding individualized treatment and follow-up management. However, there were some limitations concerning this signature. Patient cohorts were retrospectively collected and sample size was limited in select cohort. The efficacy of this prognostic signature should be further validated using more independent cohorts before it could be applied into the clinic. Moreover, in addition to EGFR, detailed molecular functions of FADD and PARK2 remain underexplored in HNSCC.

Conclusions

In conclusion, we developed and validated a novel 3-ARGs based prognostic signature for HNSCC via an integrative bioinformatics approach. This signature might have translational potentials to incorporate into routine clinical regimes upon its further validation and optimization. These findings support that autophagy critically boosts HNSCC tumorigenesis and aberration of autophagy-related genes or pathways could serve as novel diagnostic and prognostic biomarkers.

Abbreviations

HNSCC: head neck squamous cell carcinoma; ARGs:Autophagy-related genes; TCGA:The Cancer Genome Atlas; GEO:Gene Expression Omnibus; HADb:Human Autophagy Database; GO:Gene ontology; KEGG:Kyoto Encyclopedia of Genes and Genomes; DAVID:Database for Annotation, Visualization, and Integrated Discovery; OS:overall survival; ROC:receiver operating curve; AUC:area under the curves; HR:hazard ratio; CI:confidence interval; FC:fold change; HPV:human papillomavirus infection.

Declarations

Ethics approval and consent to participate

This article does not contain any studies with human reporters or animals performed by any of the authors.

Consent for publication

Not applicable.

Availability of data and materials

The data used to support the findings of this study are available from the corresponding author upon request.

Competing interests

All the authors declare that they have no competing interests.

Funding

This work is financially supported, in whole or in part, by National Natural Science Foundation of China (81572669, 81602386), Key Research Program in Jiangsu Province-Social Developmental Project (BE2020706), A Project Funded by the Priority Academic Program Development of Jiangsu Higher Education Institutions (2018-87), Qing-Lan Project and Jiangsu Young Medical Talent Project (QNRC2016851), Nanjing Medical University Science and Technology Development Funding Project (NMUB2019071).

Authors' contributions

Drs. YJ and YL performed data collection, bioinformatics analyses and manuscript preparation. Drs. HG, YW, YZ. SG, PZ and JC carried out data collection and statistical analyses. Prof. YW supervised the whole project and performed manuscript preparation and revision. All authors read and approved the final manuscript.

Acknowledgements

We would like to thank all participants that enrolled in the present study.

References

1. Siegel RL, Miller KD, Jemal A: **Cancer statistics, 2019**. *CA Cancer J Clin* 2019, **69**(1):7-34.
2. Leemans CR, Braakhuis BJ, Brakenhoff RH: **The molecular biology of head and neck cancer**. *Nat Rev Cancer* 2011, **11**(1):9-22.
3. Sacco AG, Cohen EE: **Current Treatment Options for Recurrent or Metastatic Head and Neck Squamous Cell Carcinoma**. *J Clin Oncol* 2015, **33**(29):3305-3313.
4. Argiris A, Harrington KJ, Tahara M, Schulten J, Chomette P, Ferreira Castro A, Licitra L: **Evidence-Based Treatment Options in Recurrent and/or Metastatic Squamous Cell Carcinoma of the Head and Neck**. *Front Oncol* 2017, **7**:72.
5. Carvalho AL, Nishimoto IN, Califano JA, Kowalski LP: **Trends in incidence and prognosis for head and neck cancer in the United States: a site-specific analysis of the SEER database**. *Int J Cancer* 2005, **114**(5):806-816.
6. Budach V, Tinhofer I: **Novel prognostic clinical factors and biomarkers for outcome prediction in head and neck cancer: a systematic review**. *Lancet Oncol* 2019, **20**(6):e313-e326.
7. Ravanan P, Srikumar IF, Talwar P: **Autophagy: The spotlight for cellular stress responses**. *Life Sci* 2017, **188**:53-67.
8. Towers CG, Thorburn A: **Therapeutic Targeting of Autophagy**. *EBioMedicine* 2016, **14**:15-23.
9. Jiang P, Mizushima N: **Autophagy and human diseases**. *Cell Res* 2014, **24**(1):69-79.
10. Guo JY, Xia B, White E: **Autophagy-mediated tumor promotion**. *Cell* 2013, **155**(6):1216-1219.
11. Martinet W, Agostinis P, Vanhoecke B, Dewaele M, De Meyer GR: **Autophagy in disease: a double-edged sword with therapeutic potential**. *Clin Sci (Lond)* 2009, **116**(9):697-712.
12. Choi AM, Ryter SW, Levine B: **Autophagy in human health and disease**. *N Engl J Med* 2013, **368**(19):1845-1846.
13. Mowers EE, Sharifi MN, Macleod KF: **Functions of autophagy in the tumor microenvironment and cancer metastasis**. *FEBS J* 2018, **285**(10):1751-1766.
14. Su Z, Yang Z, Xu Y, Chen Y, Yu Q: **Apoptosis, autophagy, necroptosis, and cancer metastasis**. *Mol Cancer* 2015, **14**:48.

15. Mowers EE, Sharifi MN, Macleod KF: **Autophagy in cancer metastasis**. *Oncogene* 2017, **36**(12):1619-1630.
16. Liu JL, Chen FF, Lung J, Lo CH, Lee FH, Lu YC, Hung CH: **Prognostic significance of p62/SQSTM1 subcellular localization and LC3B in oral squamous cell carcinoma**. *Br J Cancer* 2014, **111**(5):944-954.
17. Sakakura K, Takahashi H, Kaira K, Toyoda M, Oyama T, Chikamatsu K: **Immunological significance of the accumulation of autophagy components in oral squamous cell carcinoma**. *Cancer Sci* 2015, **106**(1):1-8.
18. Liu Y, Wu L, Ao H, Zhao M, Leng X, Liu M, Ma J, Zhu J: **Prognostic implications of autophagy-associated gene signatures in non-small cell lung cancer**. *Aging (Albany NY)* 2019, **11**(23):11440-11462.
19. Gu Y, Li P, Peng F, Zhang M, Zhang Y, Liang H, Zhao W, Qi L, Wang H, Wang C *et al*: **Autophagy-related prognostic signature for breast cancer**. *Mol Carcinog* 2016, **55**(3):292-299.
20. Rothenberg SM, Ellisen LW: **The molecular pathogenesis of head and neck squamous cell carcinoma**. *J Clin Invest* 2012, **122**(6):1951-1957.
21. Zhang S, Wu X, Diao P, Wang C, Wang D, Li S, Wang Y, Cheng J: **Identification of a prognostic alternative splicing signature in oral squamous cell carcinoma**. *J Cell Physiol* 2020, **235**(5):4804-4813.
22. Wang Y, Zhao W, Xiao Z, Guan G, Liu X, Zhuang M: **A risk signature with four autophagy-related genes for predicting survival of glioblastoma multiforme**. *J Cell Mol Med* 2020.
23. Lai J, Wang H, Pan Z, Su F: **A novel six-microRNA-based model to improve prognosis prediction of breast cancer**. *Aging (Albany NY)* 2019, **11**(2):649-662.
24. Tang DY, Ellis RA, Lovat PE: **Prognostic Impact of Autophagy Biomarkers for Cutaneous Melanoma**. *Front Oncol* 2016, **6**:236.
25. Song X, Yuan Z, Yuan H, Wang L, Ji P, Jin G, Dai J, Ma H: **ATG12 expression quantitative trait loci associated with head and neck squamous cell carcinoma risk in a Chinese Han population**. *Mol Carcinog* 2018, **57**(8):1030-1037.
26. Simpson DR, Mell LK, Cohen EE: **Targeting the PI3K/AKT/mTOR pathway in squamous cell carcinoma of the head and neck**. *Oral Oncol* 2015, **51**(4):291-298.
27. Lozy F, Cai-McRae X, Teplova I, Price S, Reddy A, Bhanot G, Ganesan S, Vazquez A, Karantza V: **ERBB2 overexpression suppresses stress-induced autophagy and renders ERBB2-induced mammary tumorigenesis independent of monoallelic Becn1 loss**. *Autophagy* 2014, **10**(4):662-676.
28. Wang Z, Gao L, Guo X, Feng C, Lian W, Deng K, Xing B: **Development and validation of a nomogram with an autophagy-related gene signature for predicting survival in patients with glioblastoma**. *Aging (Albany NY)* 2019, **11**(24):12246-12269.
29. Mo S, Dai W, Xiang W, Li Y, Feng Y, Zhang L, Li Q, Cai G: **Prognostic and predictive value of an autophagy-related signature for early relapse in stages I-III colon cancer**. *Carcinogenesis* 2019, **40**(7):861-870.

30. Amaravadi RK, Kimmelman AC, Debnath J: **Targeting Autophagy in Cancer: Recent Advances and Future Directions**. *Cancer Discov* 2019, **9**(9):1167-1181.
31. Li H, You L, Xie J, Pan H, Han W: **The roles of subcellularly located EGFR in autophagy**. *Cell Signal* 2017, **35**:223-230.
32. Sooro MA, Zhang N, Zhang P: **Targeting EGFR-mediated autophagy as a potential strategy for cancer therapy**. *Int J Cancer* 2018, **143**(9):2116-2125.
33. Kalyankrishna S, Grandis JR: **Epidermal growth factor receptor biology in head and neck cancer**. *J Clin Oncol* 2006, **24**(17):2666-2672.
34. Pattje WJ, Melchers LJ, Slagter-Menkema L, Mastik MF, Schrijvers ML, Gibcus JH, Kluin PM, Hoegen-Chouvalova O, van der Laan BF, Roodenburg JL *et al*: **FADD expression is associated with regional and distant metastasis in squamous cell carcinoma of the head and neck**. *Histopathology* 2013, **63**(2):263-270.
35. Reddy RB, Bhat AR, James BL, Govindan SV, Mathew R, Ravindra DR, Hedne N, Illiayaraja J, Kekatpure V, Khora SS *et al*: **Meta-Analyses of Microarray Datasets Identifies ANO1 and FADD as Prognostic Markers of Head and Neck Cancer**. *PLoS One* 2016, **11**(1):e0147409.
36. Cheng H, Yang X, Si H, Saleh AD, Xiao W, Coupar J, Gollin SM, Ferris RL, Issaeva N, Yarbrough WG *et al*: **Genomic and Transcriptomic Characterization Links Cell Lines with Aggressive Head and Neck Cancers**. *Cell Rep* 2018, **25**(5):1332-1345 e1335.
37. Lin DC, Xu L, Chen Y, Yan H, Hazawa M, Doan N, Said JW, Ding LW, Liu LZ, Yang H *et al*: **Genomic and Functional Analysis of the E3 Ligase PARK2 in Glioma**. *Cancer Res* 2015, **75**(9):1815-1827.
38. Yeo CW, Ng FS, Chai C, Tan JM, Koh GR, Chong YK, Koh LW, Foong CS, Sandanaraj E, Holbrook JD *et al*: **Parkin pathway activation mitigates glioma cell proliferation and predicts patient survival**. *Cancer Res* 2012, **72**(10):2543-2553.
39. Gupta A, Anjomani-Virmouni S, Koundouros N, Dimitriadi M, Choo-Wing R, Valle A, Zheng Y, Chiu YH, Agnihotri S, Zadeh G *et al*: **PARK2 Depletion Connects Energy and Oxidative Stress to PI3K/Akt Activation via PTEN S-Nitrosylation**. *Mol Cell* 2017, **65**(6):999-1013 e1017.
40. Diao P, Song Y, Ge H, Wu Y, Li J, Zhang W, Wang Y, Cheng J: **Identification of 4-lncRNA prognostic signature in head and neck squamous cell carcinoma**. *J Cell Biochem* 2019, **120**(6):10010-10020.
41. Tian S, Meng G, Zhang W: **A six-mRNA prognostic model to predict survival in head and neck squamous cell carcinoma**. *Cancer Manag Res* 2019, **11**:131-142.

Tables

Table 1. Univariate and Multivariate Cox regression analyses of 3-ARGs signature risk score and clinicopathological parameters in HNSCC

Variables	Univariate analyses		Multivariate analyses	
	HR [95% CI]	*P*	HR [95% CI]	*P*
TCGA cohort				
Age (≥60, <60)	1.291(0.981-1.700)	0.069		
Gender (male, female)	0.754(0.566-1.004)	0.054		
Smoking history category (≥3, <3)	0.802(0.606-1.062)	0.123		
Alcohol use (Yes, No)	0.978(0.734-1.304)	0.880		
Tumor size (T3-T4, T1-T2)	1.569(1.143-2.153)	**0.005**	1.843(1.030-3.298)	**0.039**
Pathological grade (III-IV, I-II)	1.743(1.177-2.580)	**0.006**	1.658(0.925-2.974)	0.090
Cervical node metastasis (N+, N0)	1.383(1.039-1.842)	**0.026**	1.212(0.831-1.769)	0.319
Clinical stage (III-IV, I-II)	1.257(0.901-1.753)	0.178	0.501(0.288-0.871)	**0.014**
Risk score (High, Low)	1.845(1.410-2.416)	**<0.001**	1.735(1.282-2.348)	**<0.001**

HR, hazard ratio; CI, confidence interval.

Figures

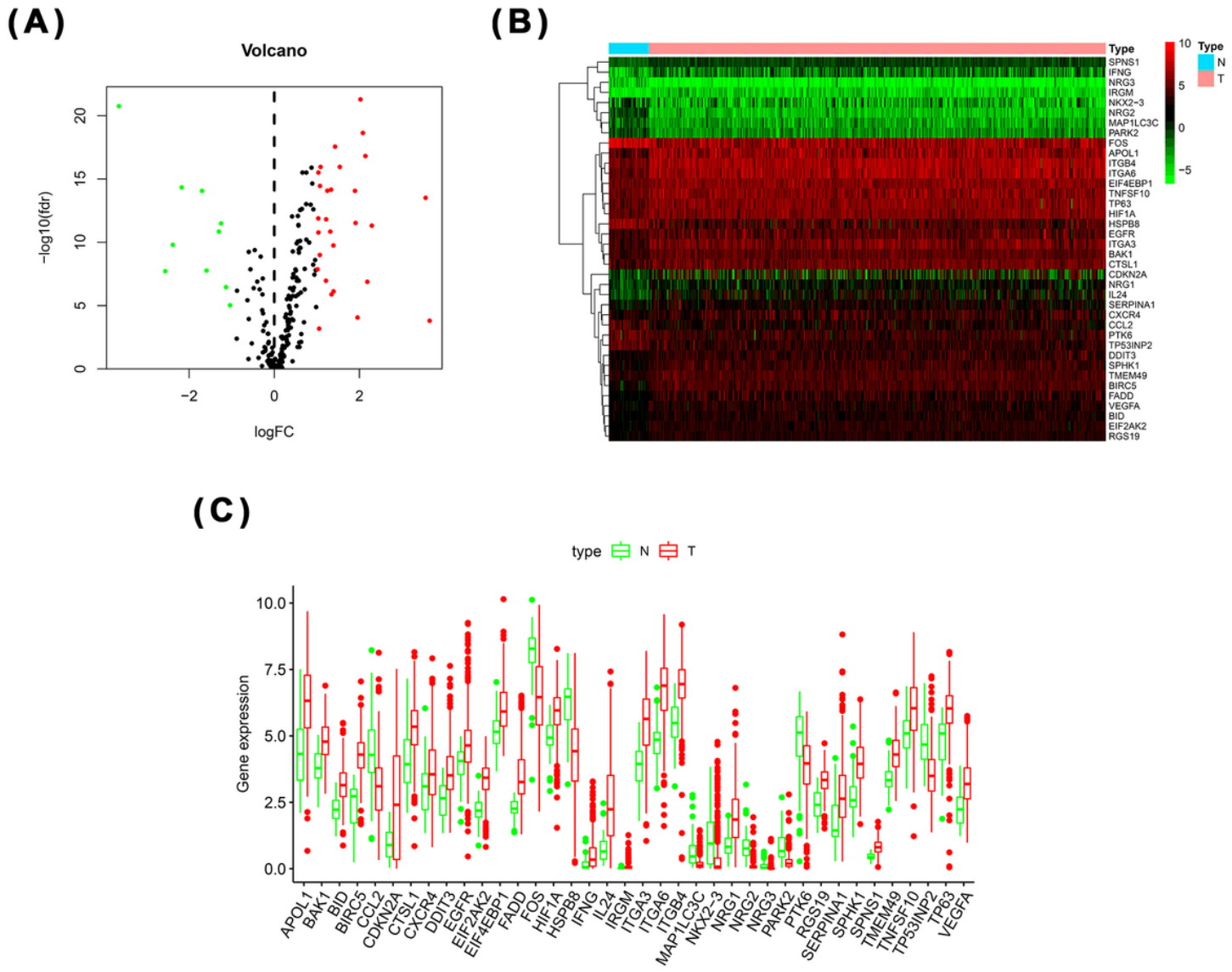

Figure 1

Identification of differentially expressed autophagy-related genes (ARGs) between HNSCC and non-tumor counterparts. A: The volcano plot for ARGs retrieved from the TCGA data portal. Red indicates high expression and green low expression. Black shows those genes showed no difference between HNSCC and non-tumor tissues. B: Hierarchical clustering of differentially expressed ARGs. C: The expression patterns of 38 ARGs in HNSCC and non-tumor samples were shown. Each red dot represents tumor samples and green represents non-tumor samples.

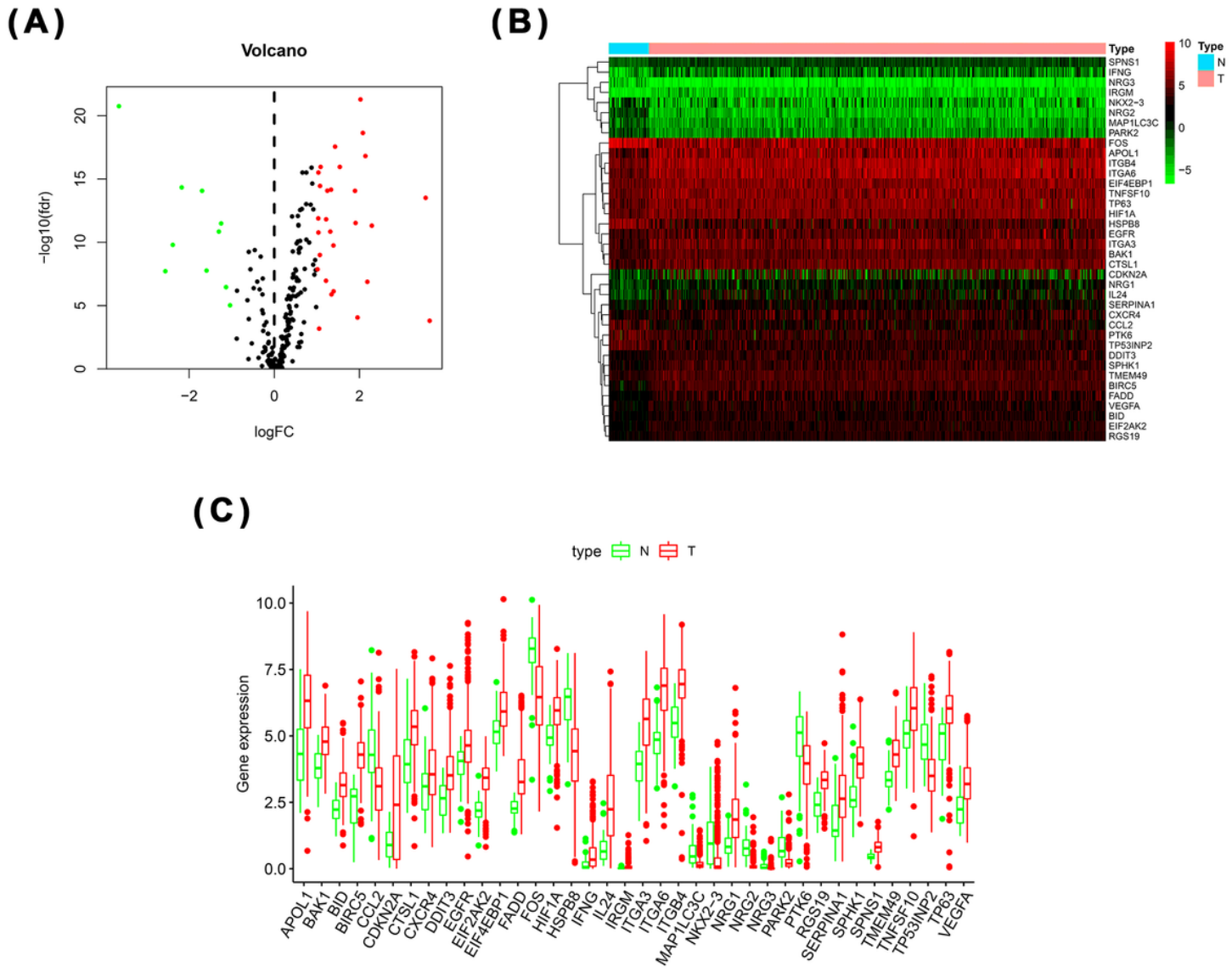

Figure 1

Identification of differentially expressed autophagy-related genes (ARGs) between HNSCC and non-tumor counterparts. A: The volcano plot for ARGs retrieved from the TCGA data portal. Red indicates high expression and green low expression. Black shows those genes showed no difference between HNSCC and non-tumor tissues. B: Hierarchical clustering of differentially expressed ARGs. C: The expression patterns of 38 ARGs in HNSCC and non-tumor samples were shown. Each red dot represents tumor samples and green represents non-tumor samples.

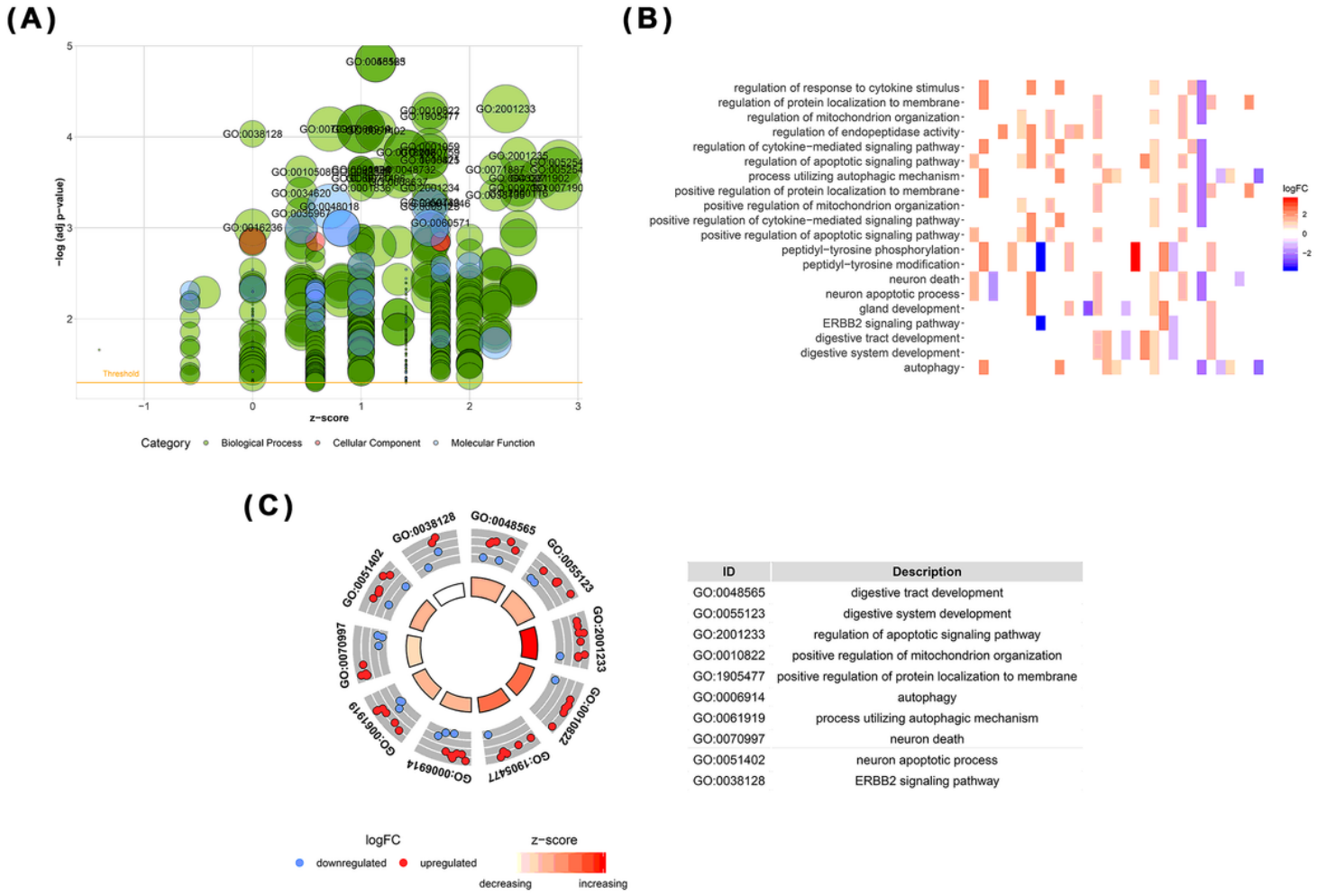

ID	Description
GO:0048565	digestive tract development
GO:0055123	digestive system development
GO:2001233	regulation of apoptotic signaling pathway
GO:0010822	positive regulation of mitochondrion organization
GO:1905477	positive regulation of protein localization to membrane
GO:0006914	autophagy
GO:0061919	process utilizing autophagic mechanism
GO:0070997	neuron death
GO:0051402	neuron apoptotic process
GO:0038128	ERBB2 signaling pathway

Figure 2

Functional annotations of differentially expressed ARGs in HNSCC A: The bubble plot of enriched gene ontology (GO) terms. The z-score is assigned to the X-axis, and the negative logarithm of the P value to the Y-axis, as in the barplot (the higher the more significant). The size of the displayed circles is proportional to the number of genes assigned to the term. Green circles correspond to the biological process, red indicates the cellular component, and blue shows the molecular function category. B: The heatmap of the relationship between ARGs and terms. The color of each block depends on the logFC values. C: The outer circle shows a scatter plot for each term of the logFC of the assigned genes. Red circles display up-regulation, and blue ones down-regulation.

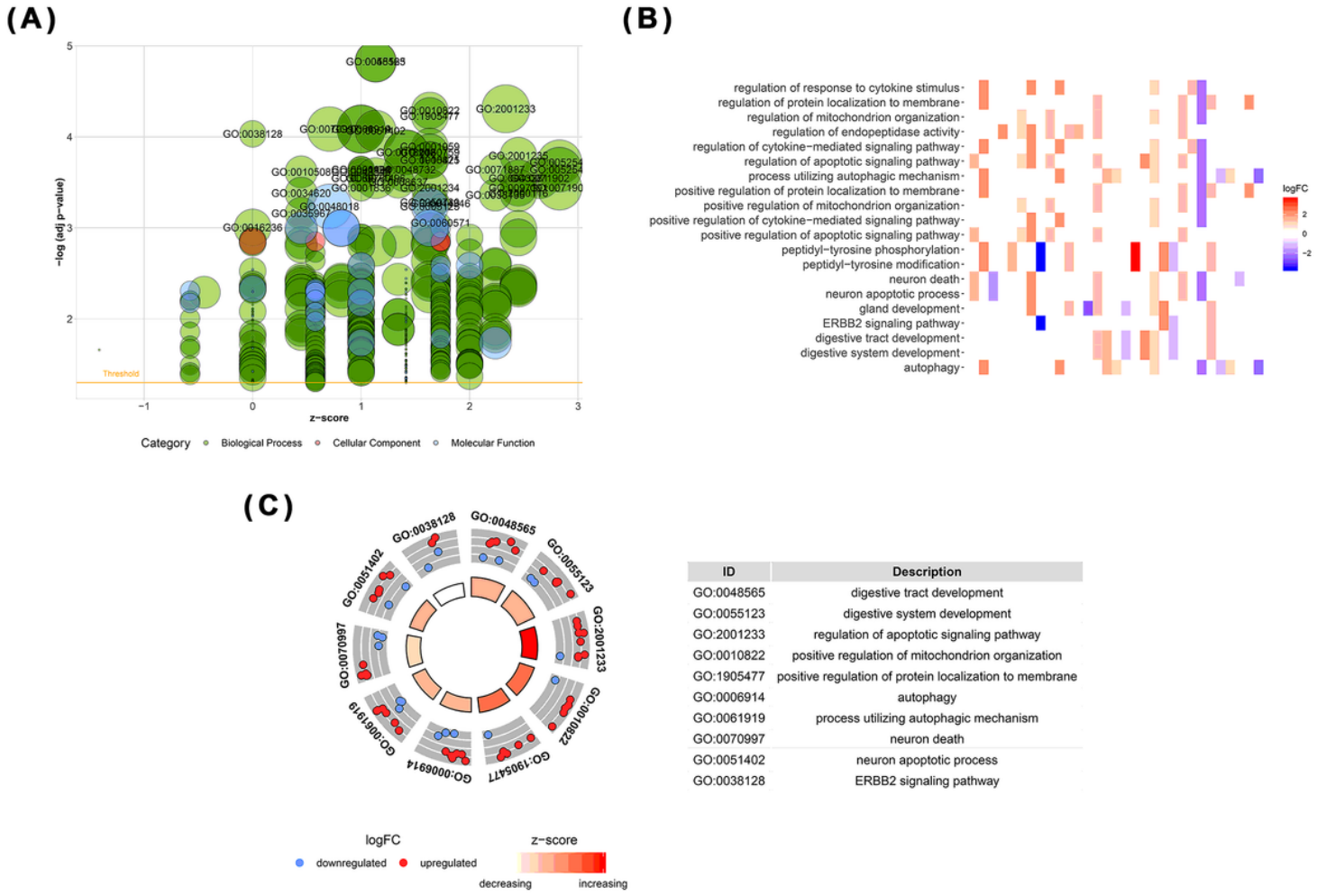

ID	Description
GO:0048565	digestive tract development
GO:0055123	digestive system development
GO:2001233	regulation of apoptotic signaling pathway
GO:0010822	positive regulation of mitochondrion organization
GO:1905477	positive regulation of protein localization to membrane
GO:0006914	autophagy
GO:0061919	process utilizing autophagic mechanism
GO:0070997	neuron death
GO:0051402	neuron apoptotic process
GO:0038128	ERBB2 signaling pathway

Figure 2

Functional annotations of differentially expressed ARGs in HNSCC A: The bubble plot of enriched gene ontology (GO) terms. The z-score is assigned to the X-axis, and the negative logarithm of the P value to the Y-axis, as in the barplot (the higher the more significant). The size of the displayed circles is proportional to the number of genes assigned to the term. Green circles correspond to the biological process, red indicates the cellular component, and blue shows the molecular function category. B: The heatmap of the relationship between ARGs and terms. The color of each block depends on the logFC values. C: The outer circle shows a scatter plot for each term of the logFC of the assigned genes. Red circles display up-regulation, and blue ones down-regulation.

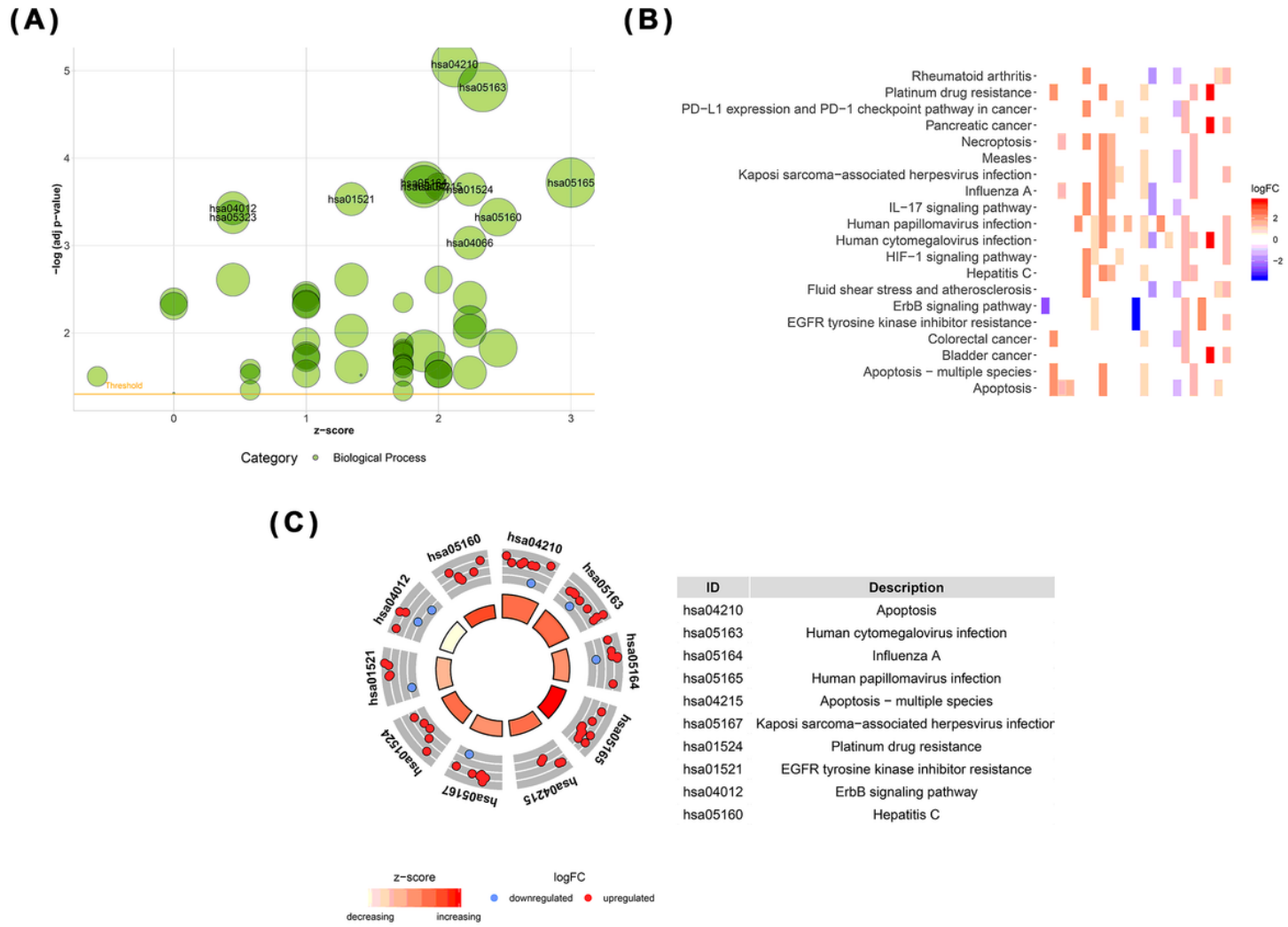

Figure 3

KEGG pathway analysis of differentially expressed ARGs in HNSCC A: The bubble plot of enriched KEGG terms. The z-score is assigned to the X-axis, and the negative logarithm of the P value to the Y-axis, as in the barplot (the higher the more significant). The size of the displayed circles is proportional to the number of genes assigned to the term. B: The heatmap of the relationship between ARGs and pathways. The color of each block depends on the logFC values. C: The outer circle shows a scatter plot for each term of the logFC of the assigned genes. Red circles display up-regulation, and blue ones down-regulation.

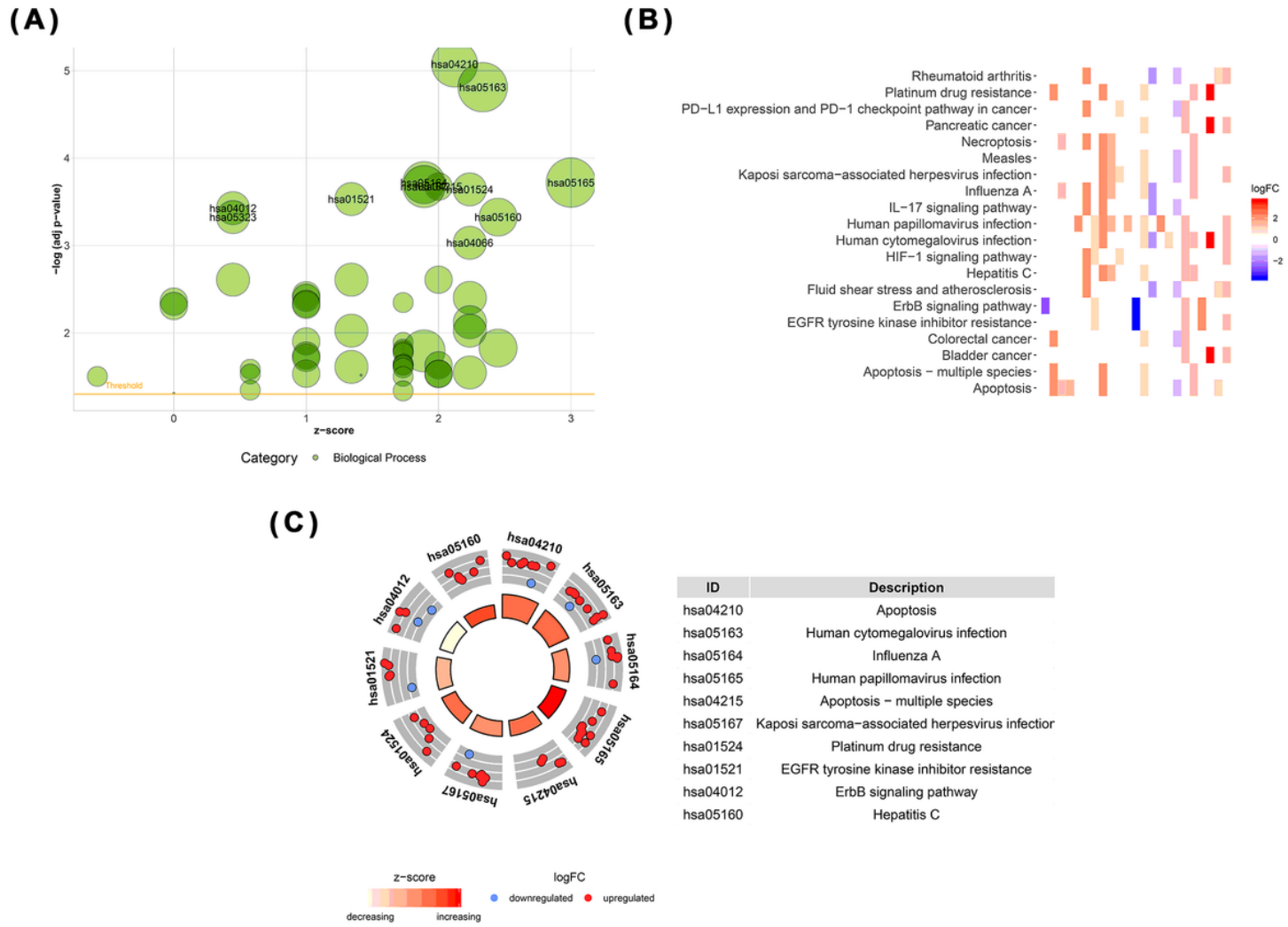

Figure 3

KEGG pathway analysis of differentially expressed ARGs in HNSCC A: The bubble plot of enriched KEGG terms. The z-score is assigned to the X-axis, and the negative logarithm of the P value to the Y-axis, as in the barplot (the higher the more significant). The size of the displayed circles is proportional to the number of genes assigned to the term. B: The heatmap of the relationship between ARGs and pathways. The color of each block depends on the logFC values. C: The outer circle shows a scatter plot for each term of the logFC of the assigned genes. Red circles display up-regulation, and blue ones down-regulation.

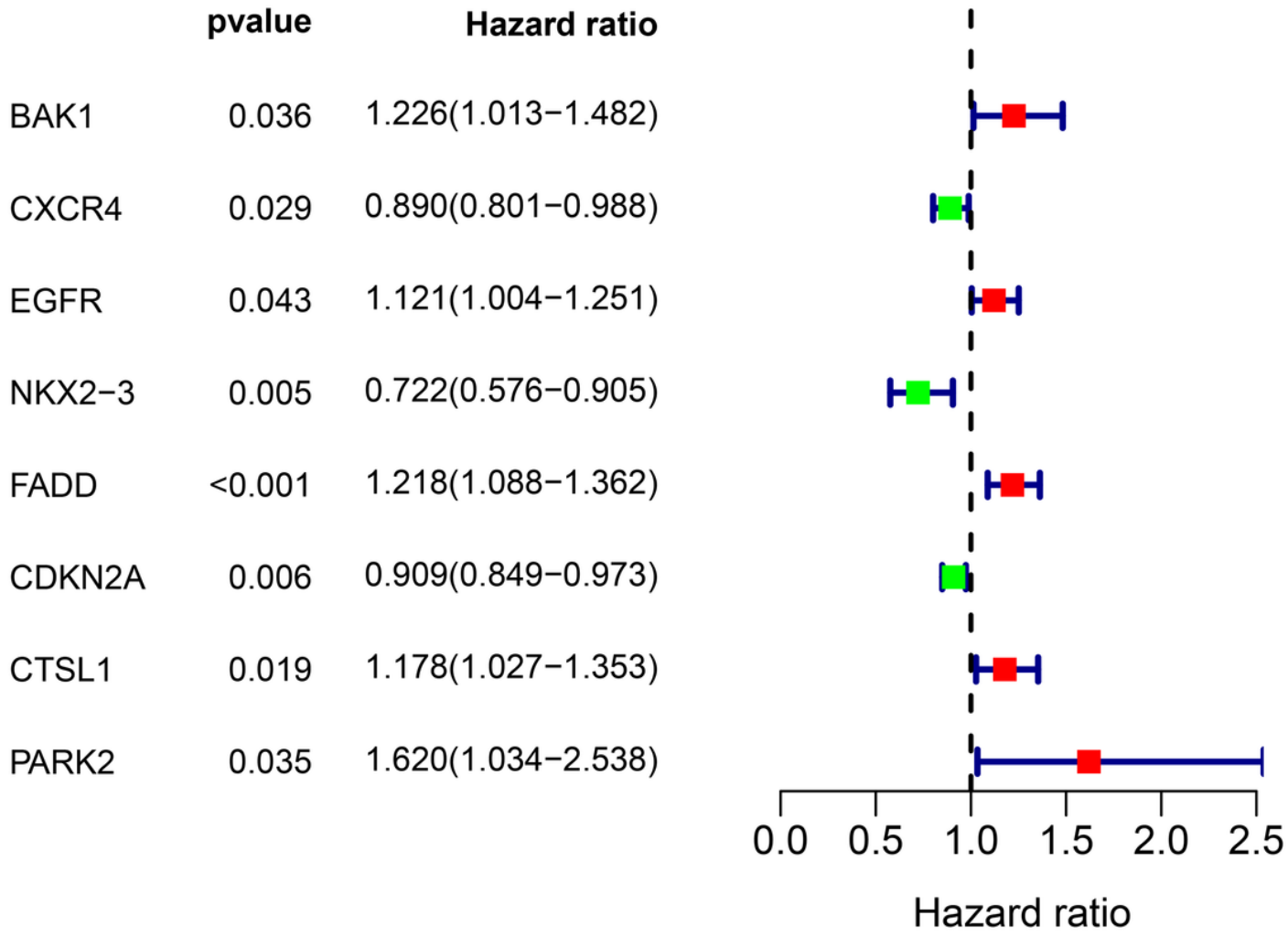

Figure 4

Univariate Cox regression analyses of ARGs with prognostic potential in TCGA-HNSCC cohort. The forest plot of 8 ARGs associated with overall survival was shown. Genes with P values less than 0.05 are considered with prognostic values.

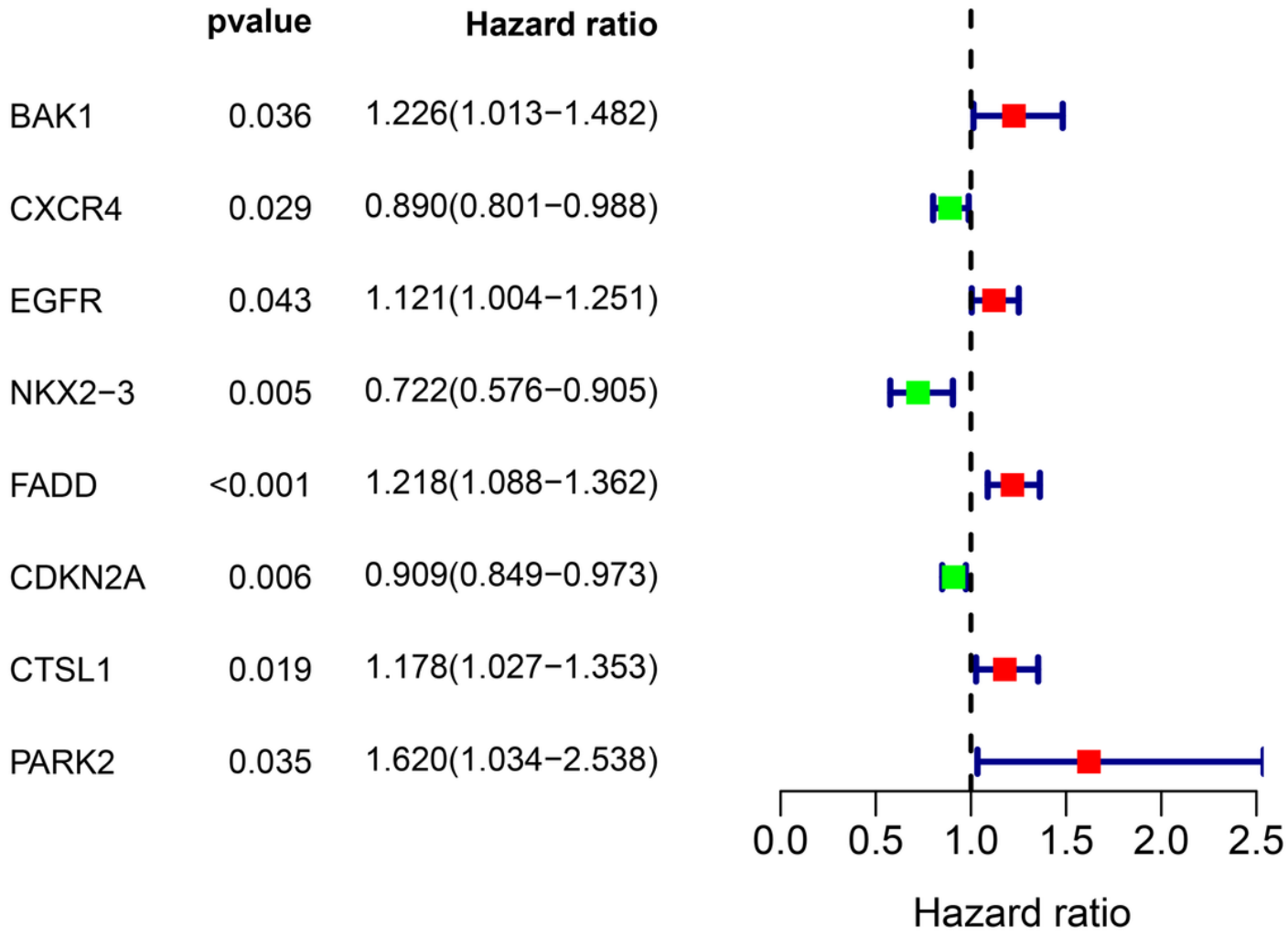

Figure 4

Univariate Cox regression analyses of ARGs with prognostic potential in TCGA-HNSCC cohort. The forest plot of 8 ARGs associated with overall survival was shown. Genes with P values less than 0.05 are considered with prognostic values.

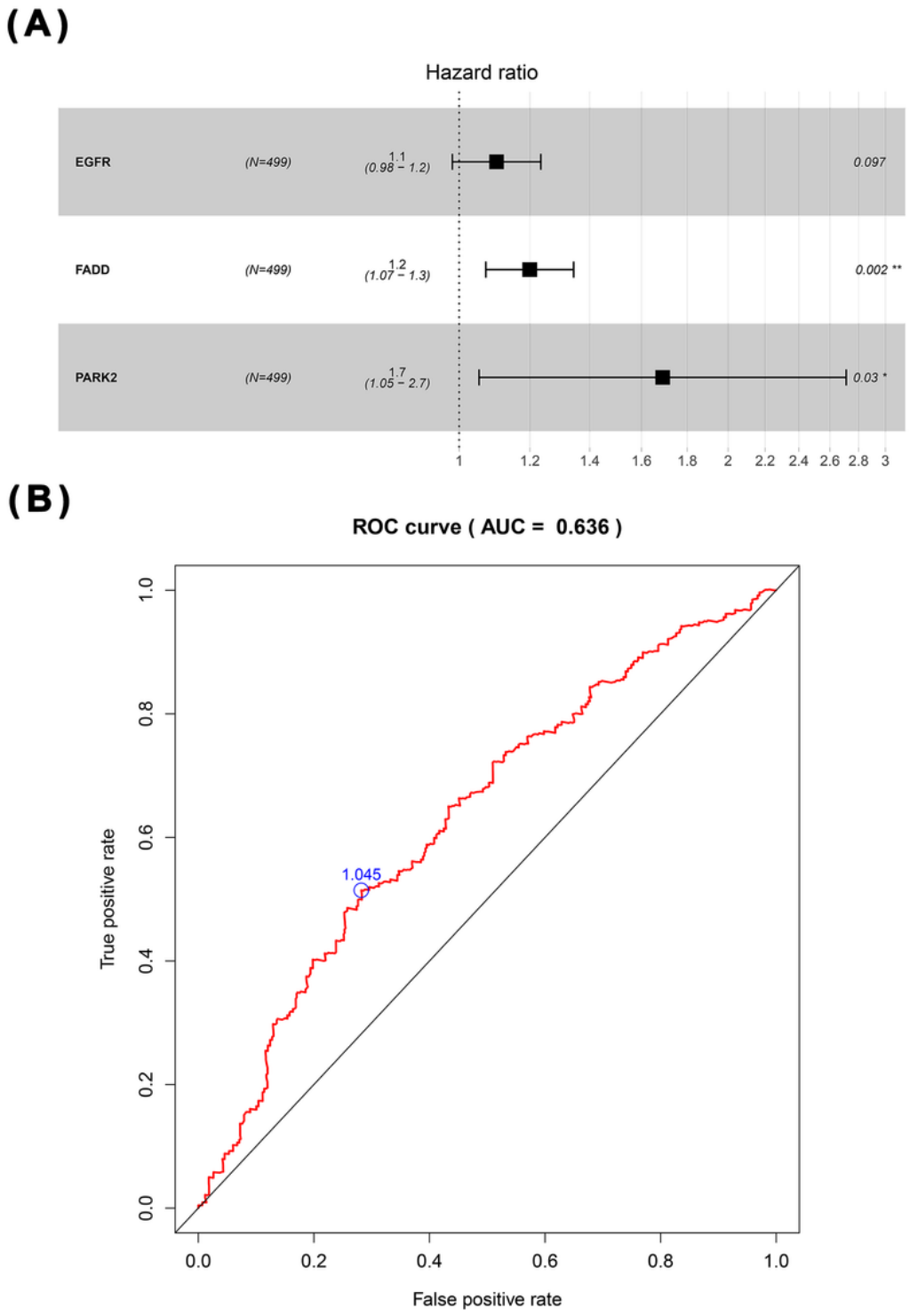

Figure 5

Identification 3-ARGs prognostic signature and its optimal cut-off value for patient stratification in the TCGA-HNSCC cohort. A: Multivariate survival analysis reveals that 3 ARGs included in our signature were independent prognostic factors associated with patient survival in the training cohort. B: ROC analysis of sensitivity and specificity of overall survival by the 3-ARGs prognostic signature based risk score. The blue dot represents the optimal cut-off values in the training cohort using ROC analysis.

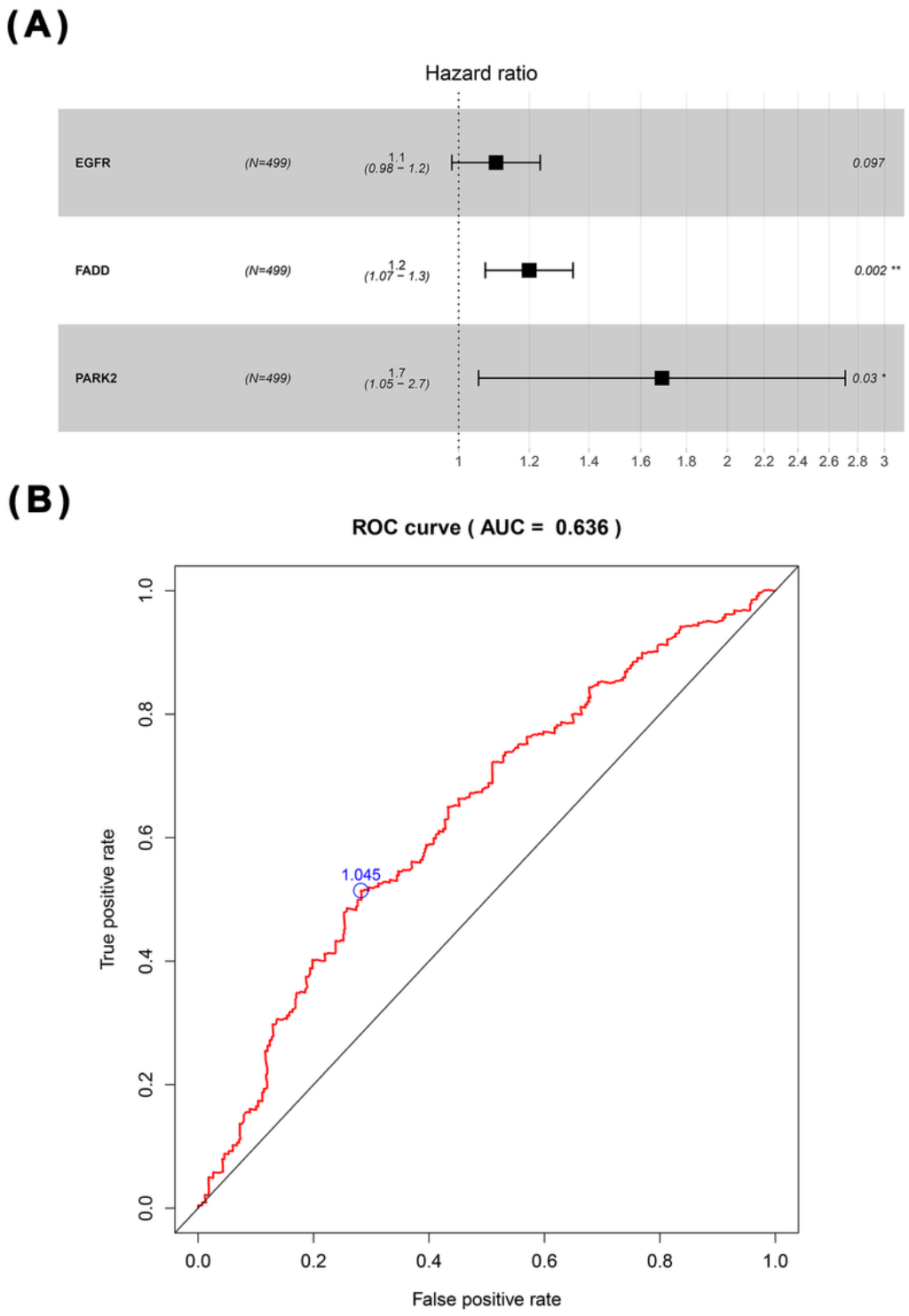

Figure 5

Identification 3-ARGs prognostic signature and its optimal cut-off value for patient stratification in the TCGA-HNSCC cohort. A: Multivariate survival analysis reveals that 3 ARGs included in our signature were independent prognostic factors associated with patient survival in the training cohort. B: ROC analysis of sensitivity and specificity of overall survival by the 3-ARGs prognostic signature based risk score. The blue dot represents the optimal cut-off values in the training cohort using ROC analysis.

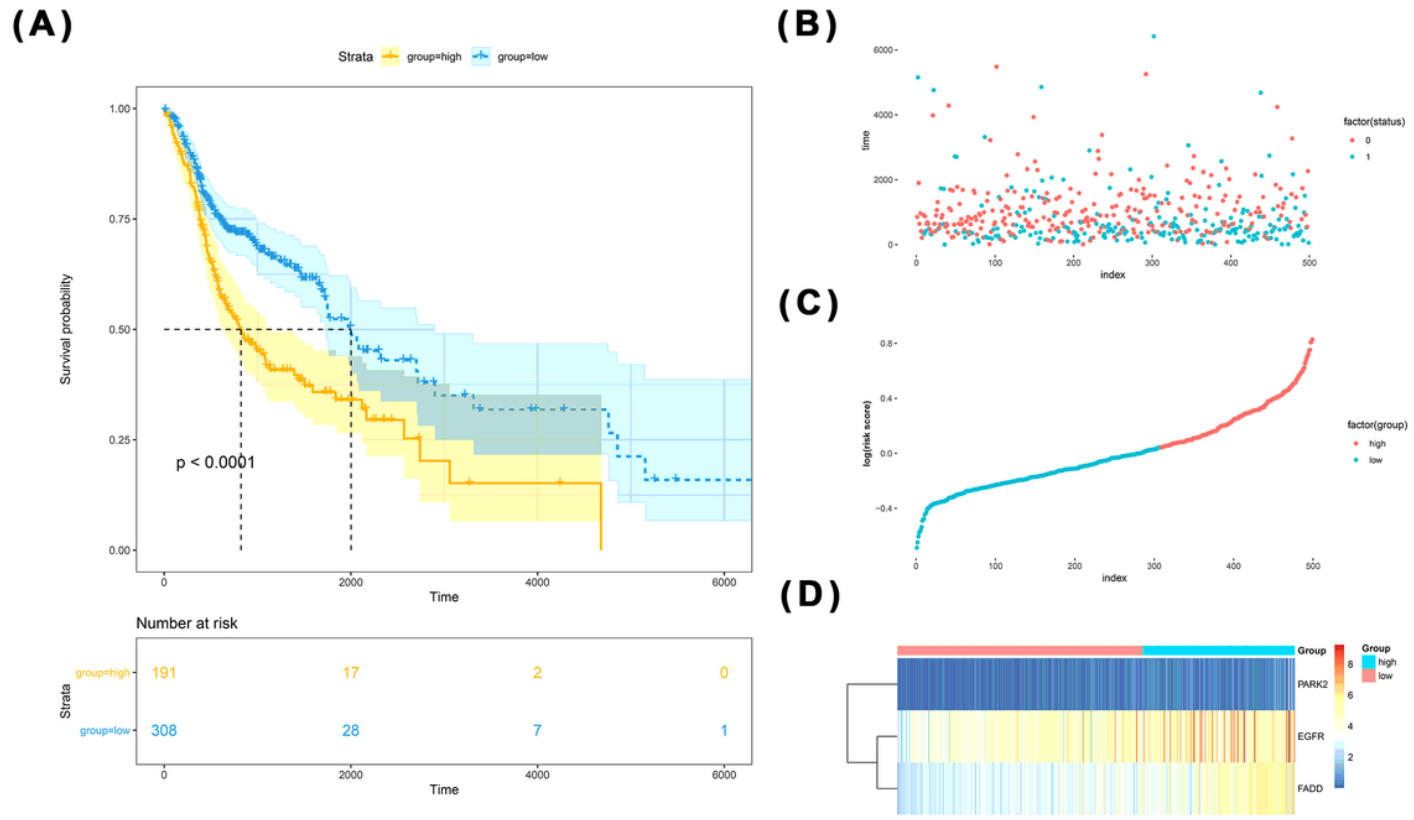

Figure 6

Risk score based on 3-ARGs prognostic signature significantly associates with patient survival. A: The Kaplan-Meier analyses of overall survival in patients from training cohort stratified by the 3-ARGs signature risk score. P values were calculated by the Log-rank test. B: Survival status of patients with HNSCC in the training cohort (TCGA-HNSCC). C: Patient subgroups with high and low risk score were classified by the optimal cut-off values. D: Distribution of a high or low risk score and individual ARG expression profiles in the training cohort were shown.

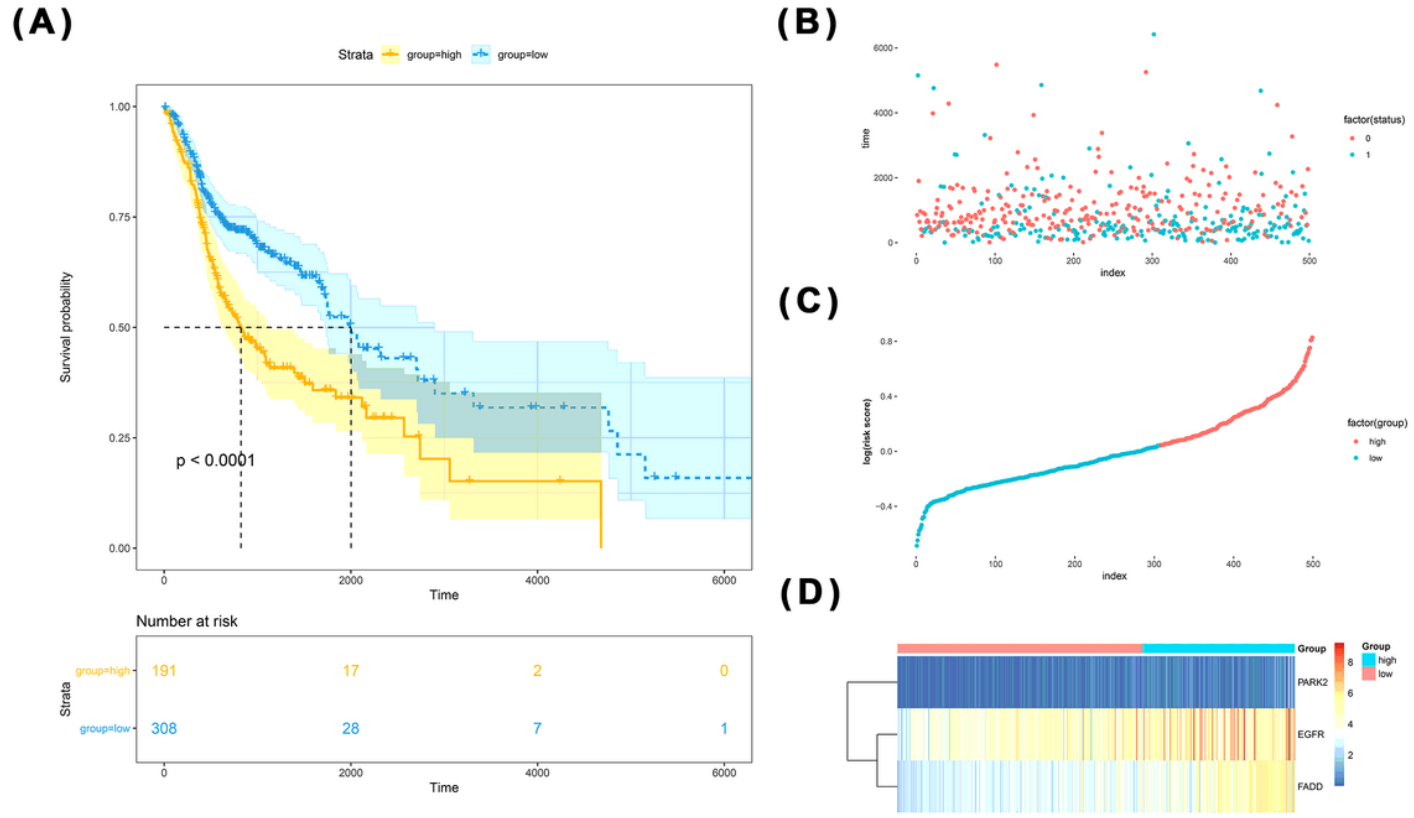

Figure 6

Risk score based on 3-ARGs prognostic signature significantly associates with patient survival. A: The Kaplan-Meier analyses of overall survival in patients from training cohort stratified by the 3-ARGs signature risk score. P values were calculated by the Log-rank test. B: Survival status of patients with HNSCC in the training cohort (TCGA-HNSCC). C: Patient subgroups with high and low risk score were classified by the optimal cut-off values. D: Distribution of a high or low risk score and individual ARG expression profiles in the training cohort were shown.

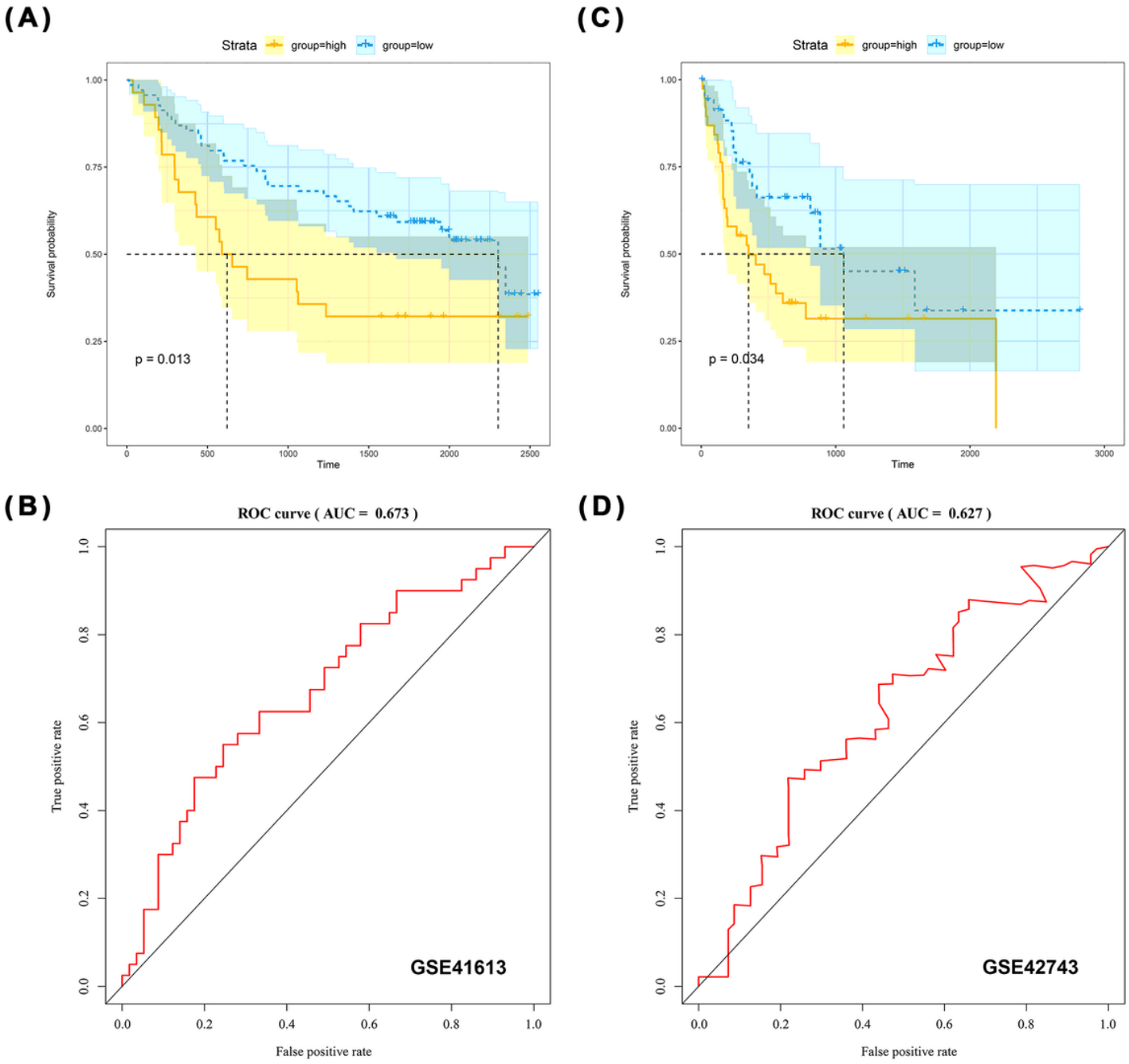

Figure 7

Verification of 3-ARGs signature in two external independent HNSCC cohorts A, C: The Kaplan-Meier analyses of overall survival in patients from the GSE41613 (A) and GSE42743 (C) dataset stratified by the 3-ARGs signature risk score. The high-risk and low-risk subgroups were divided by the optimal cut-off values. P values were calculated by the Log-rank test. B, D: ROC curves and AUC were used to estimate the sensitivity and specificity of 3-ARGs signature in the prognostic prediction of overall survival (OS) based on the GSE41613 (B) and GSE42743 (D) dataset.

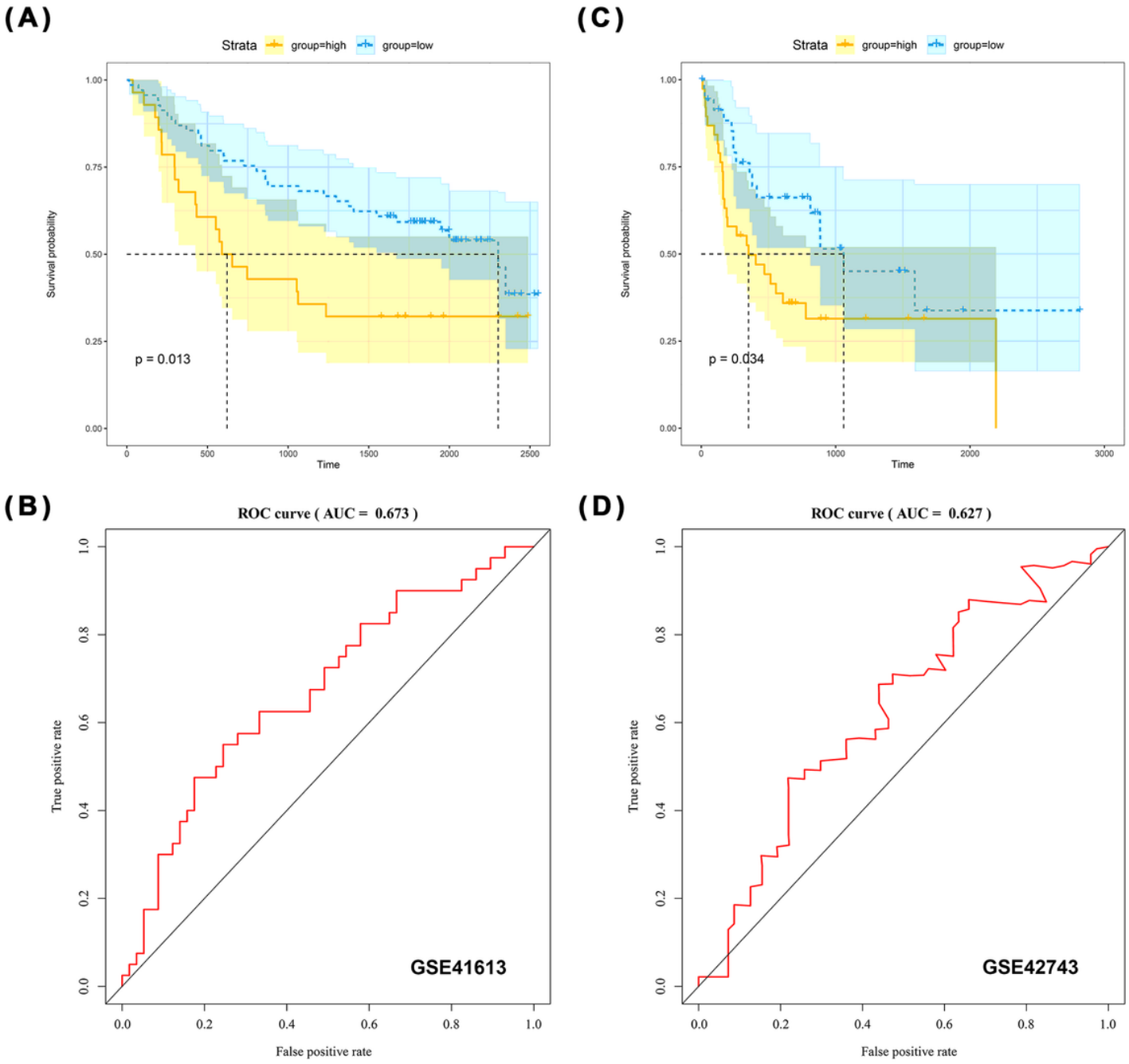

Figure 7

Verification of 3-ARGs signature in two external independent HNSCC cohorts A, C: The Kaplan-Meier analyses of overall survival in patients from the GSE41613 (A) and GSE42743 (C) dataset stratified by the 3-ARGs signature risk score. The high-risk and low-risk subgroups were divided by the optimal cut-off values. P values were calculated by the Log-rank test. B, D: ROC curves and AUC were used to estimate the sensitivity and specificity of 3-ARGs signature in the prognostic prediction of overall survival (OS) based on the GSE41613 (B) and GSE42743 (D) dataset.

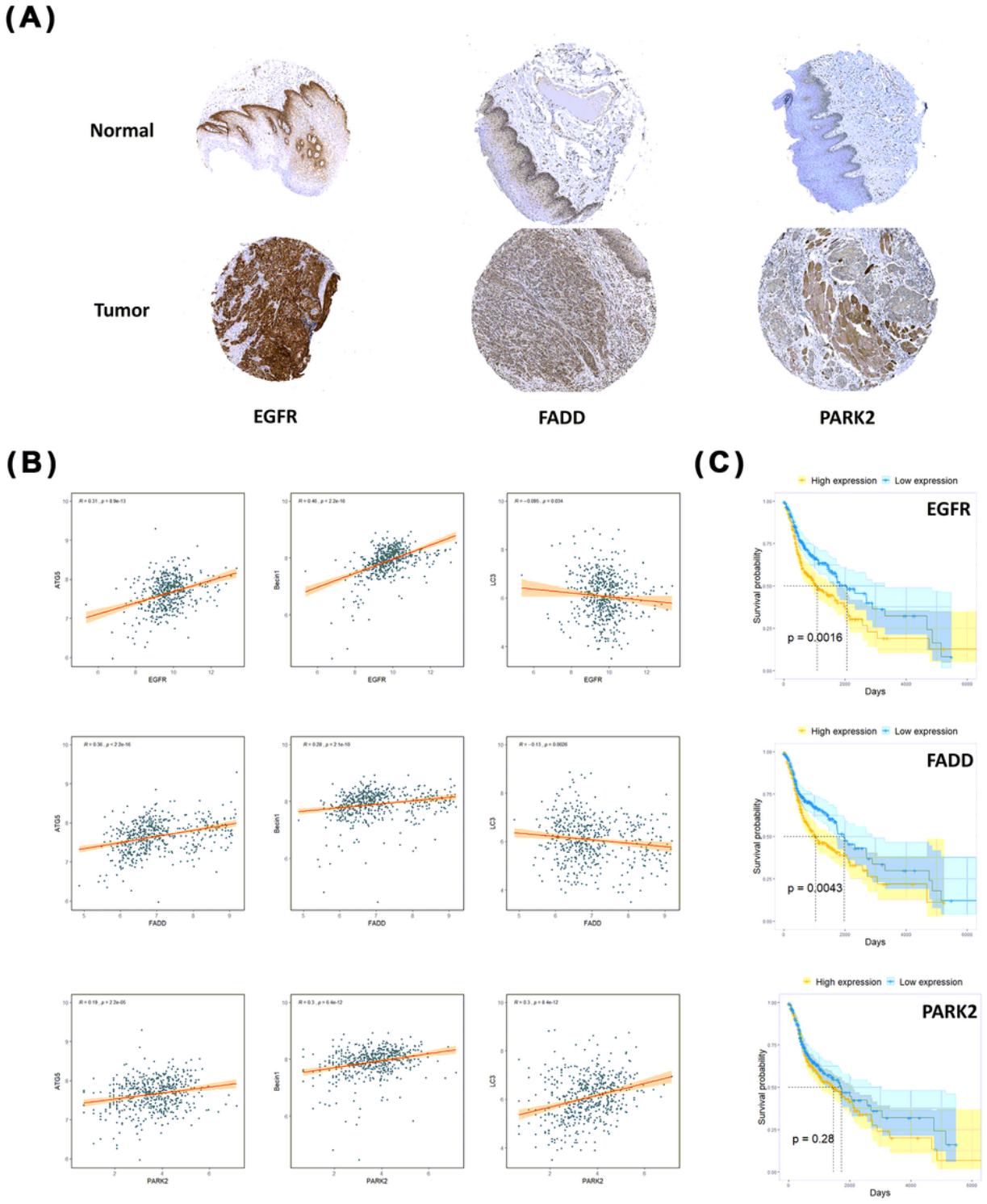

Figure 8

Expression of EGFR, FADD and PARK2 in HNSCC and their correlations with autophagy markers A: Higher expression of EGFR, FADD and PARK2 in HNSCC as compared to normal counterparts was assessed by Human Protein Atlas. B: Significant correlations between the expression of EGFR, FADD and PARK2 and three well-established autophagy markers ATG5, Beclin1 and LC3 were found in HNSCC. C: Higher

expression of EGFR and FADD significantly associated with reduced overall survival as assessed by Kaplan-Meier plots. P values were calculated by the Log-rank test.

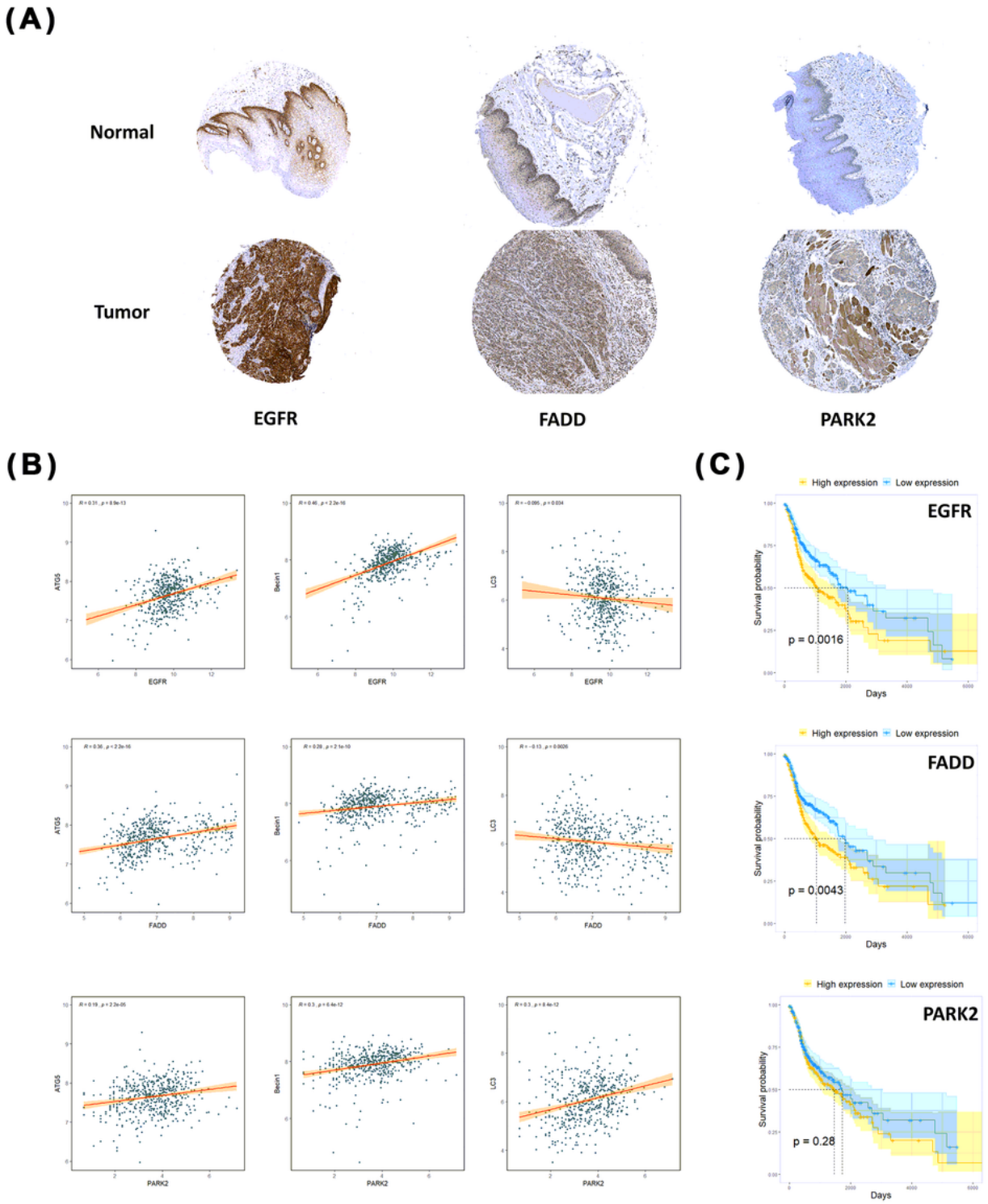

Figure 8

Expression of EGFR, FADD and PARK2 in HNSCC and their correlations with autophagy markers A: Higher expression of EGFR, FADD and PARK2 in HNSCC as compared to normal counterparts was assessed by Human Protein Atlas. B: Significant correlations between the expression of EGFR, FADD and PARK2 and

three well-established autophagy markers ATG5, Beclin1 and LC3 were found in HNSCC. C: Higher expression of EGFR and FADD significantly associated with reduced overall survival as assessed by Kaplan-Meier plots. P values were calculated by the Log-rank test.